Intra-seasonal variability in tropospheric ozone and water vapor in the tropics

J. R. Ziemke,[1,2] S. Chandra,[1,2] M. R. Schoeberl,[3] L. Froidevaux,[4] W. G. Read,[4] P. F. Levelt,[5] and P. K. Bhartia[3]

Received 11 June 2007; accepted 1 August 2007; published 5 September 2007.

[1] Nearly two years of tropospheric O_3 and H_2O data from the Aura Ozone Monitoring Instrument (OMI) and Microwave Limb Sounder (MLS) instruments are analyzed to study the characteristics of intra-seasonal oscillation (ISO) of 20–100 day periods. The analysis shows the presence of ISO signals in O_3 and H_2O throughout much of the tropics including the north Atlantic not shown in previous studies. ISO variability west of the dateline appears as a manifestation of eastward propagation of the Madden-Julian Oscillation (MJO). Time series of tropospheric O_3 and H_2O are negatively correlated throughout much of the tropics, and mostly over ocean. This suggests lofting of air from convection as a basic driving mechanism, with convection transporting low amounts of O_3 and high amounts of H_2O upwards from the boundary layer. ISO/MJO related changes in O_3 and H_2O are a major source of variability and often exceed 25% of background concentrations. **Citation:** Ziemke, J. R., S. Chandra, M. R. Schoeberl, L. Froidevaux, W. G. Read, P. F. Levelt, and P. K. Bhartia (2007), Intra-seasonal variability in tropospheric ozone and water vapor in the tropics, *Geophys. Res. Lett.*, *34*, L17804, doi:10.1029/2007GL030965.

1. Introduction

[2] An important component of atmospheric variability in both the lower and upper atmosphere is intra-seasonal oscillation (ISO) [e.g., *Kiladis et al.*, 2001; *Miyoshi and Fujiwara*, 2006, *Tian et al.*, 2007]. In the tropics, ISO is associated largely with the Madden-Julian Oscillation (MJO) which has characteristic time periods of about 30–60 days. The MJO [*Madden and Julian*, 1971, 1994] has been studied extensively because of its role in influencing air/ocean temperature, wind, convection, rainfall, outgoing longwave radiation (OLR) and several other aspects of the weather and climate system [*Lau and Chan*, 1985; *Nakazawa*, 1986; *Knutson and Kutzbach*, 1986; *Lau and Waliser*, 2004; *Zhang*, 2005, and references therein]. Meteorological perturbations caused by the MJO affect the tropical troposphere and extend from the Indian Ocean across the Pacific to at least the dateline with an eastward migration rate of about 5–10 m s^{-1}. Studies have shown that under certain conditions the MJO may affect winds and cyclonic development as far away as the tropical north Atlantic including the Caribbean Sea and Gulf of Mexico [e.g., *Park and Schubert*, 1993; *Maloney and Hartmann*, 2000; *Mo*, 2000; *Foltz and McPhaden*, 2004, 2005].

[3] Satellite measurements have shown that MJO variability in tropical latitudes is present in upper tropospheric humidity [*Sassi et al.*, 2002]. *Ziemke and Chandra* [2003a] found similar variability in tropospheric column O_3 (TCO) which was negatively correlated with upper tropospheric H_2O over ocean. The latter study indicated peak-to-peak MJO-related changes in both TCO and 215 hPa H_2O over the tropical Indian Ocean/Pacific Ocean as large as 25–50 percent of background concentrations. The negative correlation observed between TCO and H_2O suggests that convection is a basic forcing mechanism for the MJO signals in these trace gases. Deep convection associated with the MJO can transport large amounts of H_2O and low amounts O_3 from the boundary layer into the middle and upper troposphere.

[4] The MJO study of TCO and H_2O by *Ziemke and Chandra* [2003a] was based upon ozone and water vapor measurements from the Total Ozone Mapping Spectrometer (TOMS) and Microwave Limb Sounder (MLS) on the Upper Atmosphere Research Satellite (UARS). The study covered a period from October 1991 to May 1993 when measurements from the two instruments overlapped. A number of studies have shown that ISO in the atmosphere is highly variable from year to year with periods of strong activity followed by periods with weak or no activity [e.g., *Zhang*, 2005]. In addition, the ISO in meteorological parameters in the tropical Atlantic region may be only partly related to the tropical MJO which dominates tropospheric ISO over the Indian and Pacific Oceans [*Foltz and McPhaden*, 2004]. The purpose of this paper is to study the nature of the ISO in tropospheric O_3 and H_2O and its relation to the MJO based upon recent measurements of these parameters from the Ozone Monitoring Instrument (OMI) and MLS on the Aura satellite [*Schoeberl et al.*, 2004]. These measurements extend over a period of about two years from September 2004 to June 2006 and have recently been used to study the effects of the 2004 El Nino on tropospheric O_3 and H_2O [*Chandra et al.*, 2007].

2. Satellite Data and Analysis

[5] The OMI is a UV/VIS nadir solar backscatter spectrometer which provides near global coverage of total column O_3 each day with nadir spatial resolution of 13 km × 24 km [*Levelt et al.*, 2006]. The MLS measures the microwave emission lines in the frequency range 118 GHz–2.5 THz for deriving profile information of

[1]Goddard Earth Sciences and Technology, University of Maryland Baltimore County, Baltimore, Maryland, USA.
[2]Also at NASA Goddard Space Flight Center, Greenbelt, Maryland, USA.
[3]NASA Goddard Space Flight Center, Greenbelt, Maryland, USA.
[4]NASA Jet Propulsion Laboratory, Pasadena, California, USA.
[5]Royal Dutch Meteorological Institute, De Bilt, Netherlands.

0094-8276/07/2007GL030965$05.00

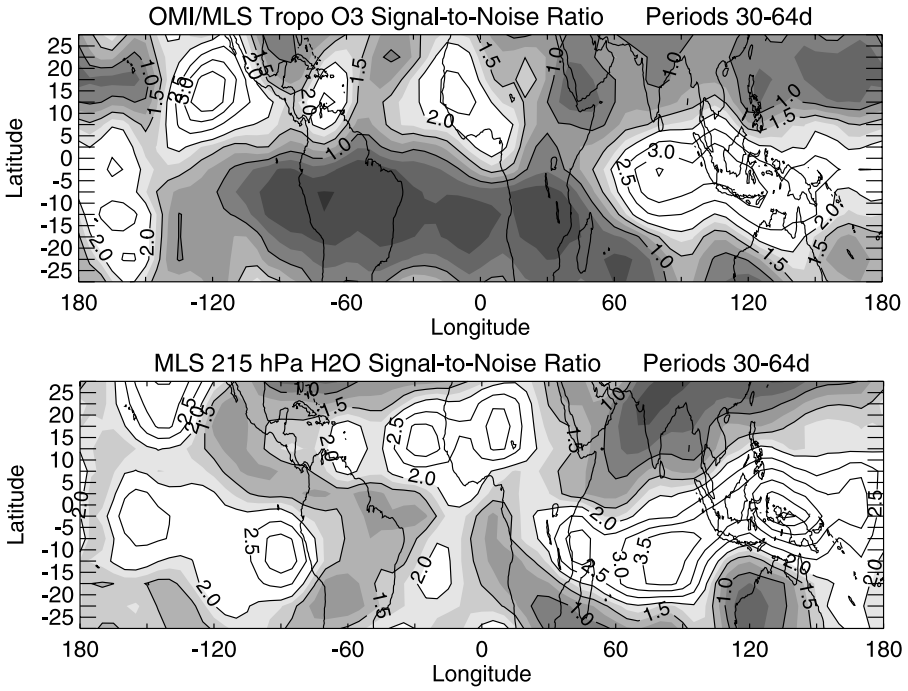

Figure 1. (top) Regions in the tropics where detected ISO signals in O_3 are statistically significant. Signal-to-noise ratio in tropospheric O_3 ISO variability is calculated for the time period September 1, 2004–May 31, 2006 (638 days). White regions with values greater than 2.1 represent power signals exceeding 95% confidence level. Contour numbers begin at 1.0 and increment by 0.5. Frequency index values 10–21 coincide with time periods 30–64 day time periods (time period in days is 638 divided by frequency index). (bottom) Same as the top plot but for 215 hPa H_2O.

several trace gases including O_3 and H_2O in the upper troposphere and middle atmosphere. These measurements are reported every 1.5 degrees of latitude along the satellite orbital track [*Waters et al.*, 2006; *Froidevaux et al.*, 2006]. The measurements from MLS and OMI are used to produce daily maps of H_2O volume mixing ratio (VMR) at several pressure levels, and stratospheric column ozone (SCO), and total column O_3. TCO is determined from total column O_3 and SCO using the OMI/MLS algorithm of *Ziemke et al.* [2006]. In producing these maps, only daytime (ascending orbit) MLS retrievals (co-located within 7 minutes with OMI) are used. All maps of O_3 and H_2O were binned to $5° \times 5°$ resolution using the 2D interpolation scheme of *Ziemke et al.* [2006].

[6] To facilitate comparison with H_2O-VMR, TCO is converted into average volume mixing ratio between the surface and the tropopause. The two ozone measurements are related by the following expression: $O_3\text{-AVMR} = 1.27 \times \text{TCO}/(P_{surface}\text{-}P_{tropopause})$ where O_3-AVMR is in parts per million by volume (ppmv), TCO is in Dobson Units (DU, 1 DU = 2.69×10^{20} molecules m^{-2}), and $P_{surface}$ and $P_{tropopause}$ are surface and tropopause pressure in hPa. $P_{tropopause}$ was determined from NCEP analyses using the 2 K-km^{-1} thermal vertical gradient criterion of the World Meteorological Organization (WMO). The typical value of $P_{tropopause}$ is about 100 hPa over most of the tropical region. As shown by *Ziemke et al.* [2006], TCO and O_3-AVMR have similar spatial patterns except in regions where changes in tropopause and terrain pressures are significant. On average, 1 DU in TCO corresponds to about 1.5 ppbv in O_3-AVMR in the tropics and about 1.7 ppbv in middle and high latitudes.

3. MJO Signal-to-Noise Ratio

[7] Since the MJO periods are typically in the range of 30–60 days, both O_3-AVMR and 215 H_2O-VMR time series from September 2004 to June 2006 were analyzed to estimate the signal-to-noise power ratio in this time range. This was determined by (1) applying a Hanning window to each daily time series followed by (2) applying a 3-point Daniell spectral estimator [e.g., *Koopmans*, 1974], and (3) determining the noise spectrum from standard first-order auto-regression of local gridded time series. Power ratios exceeding 2.1 are deemed statistically significant at the 95% confidence level. (A similar analysis was used by *Ziemke and Chandra* [2003a] for O_3 and H_2O time series from October 1991 to May 1993.) Figure 1 shows maps of signal-to-noise ratio in the 30–60 day range based on the power spectrum analysis of O_3-AVMR and 215 hPa H_2O-VMR time series. The analyses indicate regions of statistically significant signals in both O_3 and H_2O in low latitudes in the Indian Ocean and western Pacific Ocean. Statistically significant regions occur at higher latitudes in the eastern Pacific (both north and south of equator) and also extend into the north Atlantic including northern Africa. Regional differences exist between O_3 and H_2O power ratios, most notably in the eastern Pacific. Some differences are anticipated since O_3 represents tropospheric mean mixing ratio whereas H_2O measurements correspond to a fixed pressure level at 215 hPa. Temporal changes in H_2O at 215 hPa may

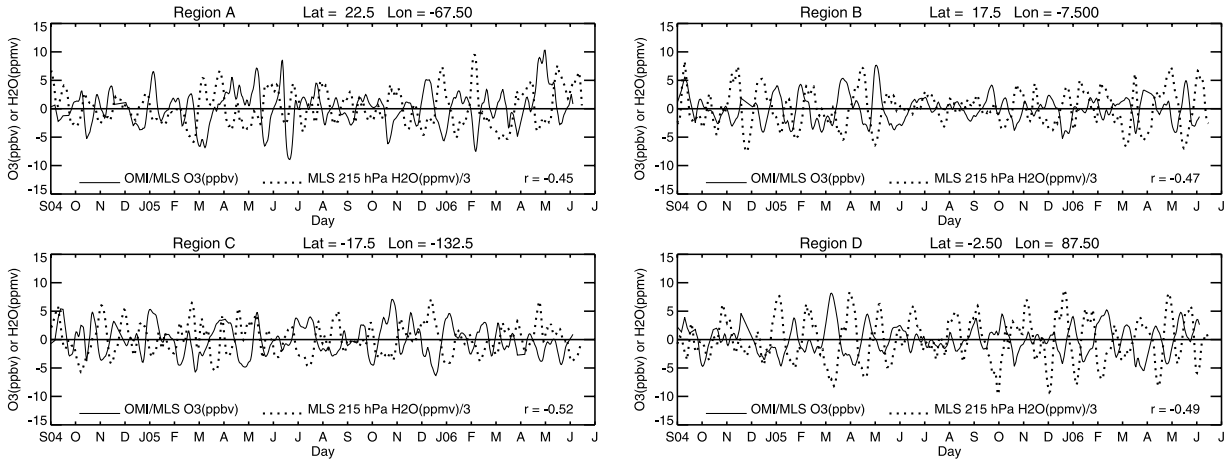

Figure 2. ISO filtered time series of O_3 (solid curves) and H_2O (dashed curves) in the north Atlantic (regions A and B in Figure 3) and Pacific (regions C and D in Figure 3).

not reflect temporal changes at other levels in the troposphere.

[8] The power spectrum analysis for tropospheric O_3 in Figure 1 (top) was also applied to SCO but did not show detectable ISO signal. The absence of ISO variability in tropical SCO was noted previously by *Ziemke and Chandra* [2003a]. Results shown in this section are similar to those obtained by *Sassi et al.* [2002] and *Ziemke and Chandra* [2003a] in the Pacific region. The current study shows evidence of significant ISO with periods in the range of 30–60 days in tropical tropospheric H_2O and O_3 in regions far distant from the MJO-related Indian Ocean and western Pacific.

4. Tropospheric O_3 and H_2O Time Series Comparisons

[9] Figure 2 compares O_3 and H_2O band-pass filtered time series at four selected locations in the Pacific and north Atlantic regions. Time series marked A and B lie in the north Atlantic while C and D lie in the Indian Ocean and eastern Pacific regions (see Figure 3). The time series were constructed using a zero-phase shift digital low-pass filter [*Stanford et al.*, 1993]. Band-pass filtered time series of 30–60 day timescale were derived by differencing 20-day and 100-day (periods at 0.5 transfer function response) low-pass filtered time series (30- and 60-day represent periods where the net filter transfer function is about 0.7.) For testing statistical significance of O_3 and H_2O cross-correlation, a Monte Carlo method was applied to estimate 95% and other confidence levels. Simulated time series of O_3 and H_2O were modeled as first-order autoregressive red noise and further band-pass filtered as the original data. For 95% confidence level (5% significance level), critical correlation magnitudes were determined to vary from 0.20 to 0.25 for measured autoregressive coefficients varying from 0.2 to 0.8, respectively (i.e., noise time series were modeled from autoregressive coefficient α as $x(t) = \alpha x(t-1)$ where t is day index). As a conservative measure only correlation amplitudes exceeding 0.25 are considered statistically significant at 95% confidence level. Similarly, values exceeding 0.32 and 0.40 are deemed significant at 99% and 99.9% confidence level, respectively.

[10] The O_3 and H_2O time series in all four cases in Figure 2 are negatively correlated with correlation amplitudes of about 0.5. Correlation between O_3 and H_2O time

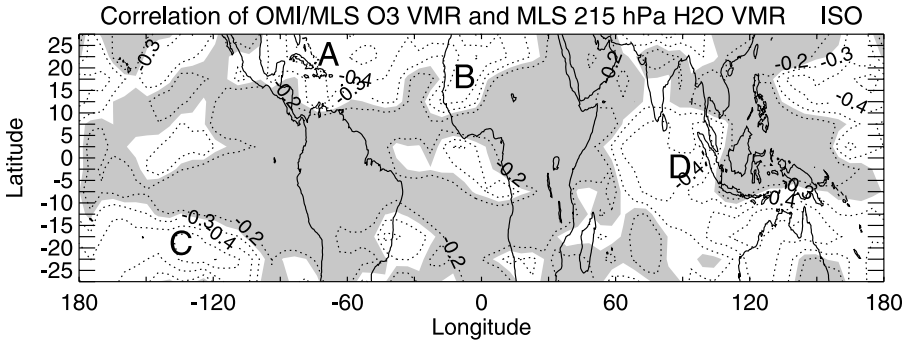

Figure 3. Map of cross-correlation between ISO-filtered O_3 and H_2O daily data for September 1, 2004–May 31, 2006. Both positive and negative correlations are plotted for correlation magnitudes >0.2, but only negative correlations have magnitudes >0.2. Regions where correlation is not significant at 95% confidence level are shaded gray. Letters A-D designate selected time series comparison locations, two of them over the north Atlantic and two in the Pacific (see text). Approximately 28% and 14% of total map area has correlation magnitudes >0.25 and 0.32, respectively – that is, passing local 95% and 99% confidence level tests.

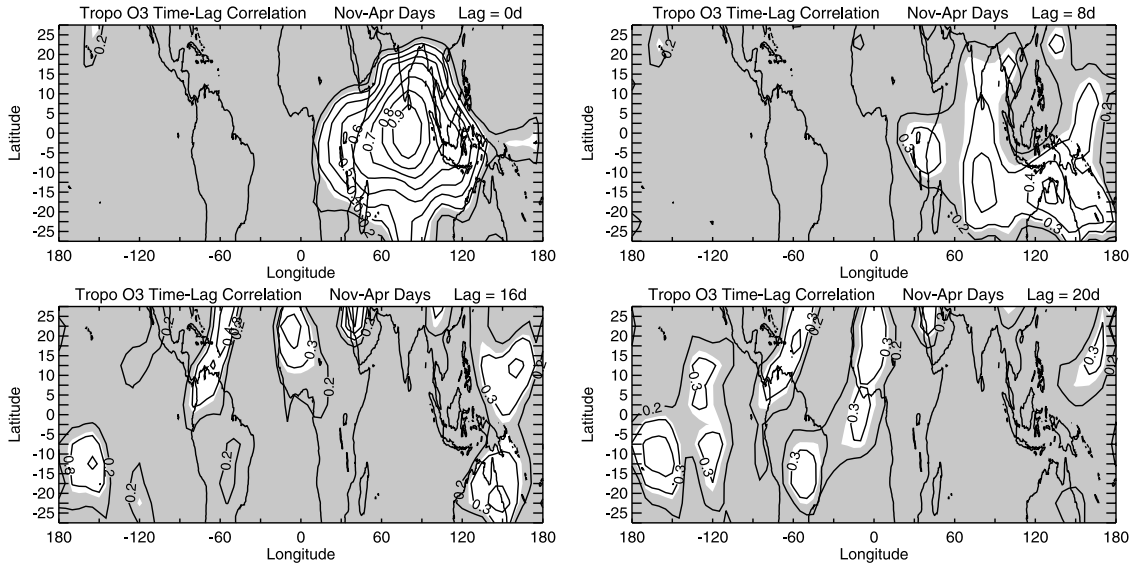

Figure 4. Time-lag correlation plots of ISO-filtered tropospheric O_3 with reference time series located along the equator at longitude 82.5°E (i.e., in the center of large equatorial MJO signal-to-noise; see Figure 1 (top)). The selected time lags are zero, eight, 16, and 20 days. Positive time lag represents local time series values at later time, relative to the reference time series. White shaded regions are statistically significant at 95% confidence level. All four maps also pass 95% statistical field significance testing.

series covering regions out to the subtropics is shown in Figure 3. Regions where correlation is not significant at 95% confidence level are shaded gray. All statistically significant correlation is negative and occurs mostly over ocean, suggesting that regional changes in SST and lofting of air mass from convection events may be a main source of observed negative correlation.

5. Eastward Propagation of ISO Signals

[11] The presence of ISO signals in O_3 and H_2O and their propagation from the Indian Ocean to the dateline can be inferred from Hovmoller diagrams (not shown) as in the work by *Ziemke and Chandra* [2003a]. The phase characteristics are similar to those from outgoing longwave radiation (OLR) diagrams (e.g., see National Oceanic and Atmospheric Administration webpage http://www.cpc.noaa.gov/products/precip/CWlink/MJO/mjo.shtml). These parameters all show relatively stronger signals during boreal winter and spring months west of the dateline. The eastward propagation of ISO signals in tropospheric O_3-AVMR is illustrated in Figure 4 which shows time-lag correlation of 30–60 day filtered time series with a reference time series located along the equator at longitude 82.5°E in the center of large MJO signal (see Figure 1 (top)). The time series were constructed from 2005 and 2006 data from November to May. Selected time lags in Figure 4 are zero, eight, 16, and 20 days. The time lag of 20 days represents about one half of the MJO time period. Positive time lag represents local time series values at later time, relative to the reference time series. For clarity in illustrating potential propagation characteristics from the reference point region, only positive correlations are shown in Figure 4. A Monte Carlo method similar to *Livesey and Chen* [1983] was also invoked to test for statistical field significance by modeling the reference point time series as first-order autoregressive. All four maps in Figure 4 were found to pass 95% field significance.

[12] Figure 4 suggests an eastward propagation of ISO signals originating in the Indian Ocean. After 8 days, positive correlation reaches just west of the dateline, indicating an eastward migration rate $\sim$8 m s^{-1}. There is indication that MJO-related signals in these trace gases originating in the Indian Ocean may cross the dateline and reach the eastern Pacific and Atlantic regions. After 8-day time lag the correlation patterns in Figure 4 east of the dateline appear as fragmented, yet statistically significant regions extending into the north Atlantic. It is possible that the ISO signals east of the dateline including the north Atlantic are related to MJO forcing, but other sources including the North Atlantic Oscillation (NAO) [*Foltz and McPhaden*, 2004] are also known to contribute to ISO variability in the troposphere.

6. Summary

[13] Nearly two years of data from OMI and MLS on the Aura satellite were analyzed to study spatial and temporal characteristics of tropical intra-seasonal oscillation (ISO) in tropospheric O_3 and H_2O. Peak-to-peak changes in O_3 average volume mixing ratio (O_3-AVMR) related to ISO variability are $\sim$5–10 ppbv throughout much of the tropics including the north Atlantic. When compared to local background concentrations this ISO variability represents changes of up to 25% or greater. Corresponding variability in H_2O VMR at 215 hPa is comparable and is negatively correlated with changes in O_3-AVMR. The ISO signals in both tropospheric O_3 and H_2O are sizeable and should be considered when evaluating variability in these trace gases for time records longer than a few days.

[14] The features of ISO in tropospheric O_3 and H_2O are similar to those reported by *Sassi et al.* [2002] and *Ziemke and Chandra* [2003a] which were studies based upon a

much earlier TOMS and MLS data record from October 1991 to May 1993. Those studies and the current study differ with respect to the extending spread of ISO signals from the western Pacific to the tropical north Atlantic. These differences are consistent with the varying nature of ISO signals including the Madden-Julian Oscillation (MJO) in trace gases and geophysical parameters extending from the Indian Ocean to the dateline, eastern Pacific, and north Atlantic regions inferred from earlier studies.

[15] Lofting of tropospheric air mass associated with convection is a likely source for the large ISO amplitudes and negative correlation measured between tropospheric O_3 and H_2O in the tropics, particularly in the Indian Ocean and Pacific Ocean regions in association with deep convective clouds. Over the generally pollution-free oceanic regions, convection brings low concentrations of O_3 and high H_2O upwards from the boundary layer into the middle and upper troposphere and is consistent with observed anomalies in outgoing longwave radiation (OLR) flux [e.g., *Chandra et al.*, 1998]. OLR data have been used extensively to characterize tropical deep convection anomalies associated with the MJO [e.g., *Mathews*, 2000]. Other possible explanations for negative correlation between O_3 and H_2O might involve cloud-lightning NO_x (which generates O_3) along with transport effects including movement of the tropopause. Transport of low H_2O into a region may tend to increase the lifetime of O_3 and its abundance, also yielding a negative correlation relationship.

[16] It is beyond the scope of this paper to evaluate various theories and hypotheses which have been proposed to explain the spatial and temporal characteristics of ISO/MJO signals in the troposphere. For tropospheric O_3 and H_2O there are many dynamical and photochemical relationships which require extensive modeling to understand the relative importance of these processes in generating ISO/MJO variability. Numerical simulations of the MJO based upon general circulation models (GCMs) are still in an evolutionary stage [*Zhang*, 2005].

[17] The impact of MJO variability in affecting tropospheric O_3 in relation to climate change requires further study. It would be important to evaluate the inter-relationships between tropical MJO/ISO and the tropical El Nino and La Nina events in tropospheric O_3. *Ziemke and Chandra* [2003b] have shown evidence that El Nino and La Nina events are the major sources of inter-annual and climate variability in tropospheric O_3 in the tropics.

[18] **Acknowledgments.** The authors thank the Aura MLS and OMI instrument and algorithm teams for the extensive satellite measurements used in this study. OMI is a Dutch-Finnish contribution to the Aura mission. Funding for this research was provided in part by Goddard Earth Science Technology (GEST) grant NGC5-494. Work at the Jet Propulsion Laboratory, California Institute of Technology, was carried out under a contract with the National Aeronautics and Space Administration.

References

Chandra, S., J. R. Ziemke, W. Min, and W. G. Read (1998), Effects of 1997–1998 El Niño on tropospheric ozone and water vapor, *Geophys. Res. Lett.*, *25*, 3867–3870.

Chandra, S., J. R. Ziemke, M. R. Schoeberl, L. Froidevaux, W. G. Read, P. F. Levelt, and P. K. Bhartia (2007), Effects of the 2004 El Niño on tropospheric ozone and water vapor, *Geophys. Res. Lett.*, *34*, L06802, doi:10.1029/2006GL028779.

Foltz, G. R., and M. J. McPhaden (2004), The 30–70 day oscillations in the tropical Atlantic, *Geophys. Res. Lett.*, *31*, L15205, doi:10.1029/2004GL020023.

Foltz, G. R., and M. J. McPhaden (2005), Mixed layer heat balance on intraseasonal time scales in the northwestern tropical Atlantic Ocean, *J. Clim.*, *18*(20), 4168–4187.

Froidevaux, L., et al. (2006), Early validation analyses of atmospheric profiles from EOS MLS on the Aura satellite, *IEEE Trans. Geosci. Remote Sens.*, *44*(5), 1075–1092.

Kiladis, G. N., et al. (2001), Aspects of interannual and intraseasonal variability of the tropopause and lower thermosphere, *Q. J. R. Meteorol. Soc.*, *127*, 1961–1983.

Knutson, T. R., and J. E. Kutzbach (1986), Global-scale intraseasonal oscillations of outgoing longwave radiation and 250 mb zonal wind during Northern Hemisphere summer, *Mon. Weather Rev.*, *114*, 605–623.

Koopmans, L. H. (1974), *The Spectral Analysis of Time Series*, 366 pp., Elsevier, New York.

Lau, K.-M., and P. H. Chan (1985), Aspects of the 40–50 day oscillation during the northern winter as inferred from outgoing longwave radiation, *Mon. Weather Rev.*, *113*, 1889–1909.

Lau, K.-M., and D. E. Waliser (2004), *Intraseasonal Variability in the Atmosphere-Ocean Climate System*, 474 pp., Springer Praxis, New York.

Levelt, P. F., et al. (2006), The Ozone Monitoring Instrument, *IEEE Trans. Geophys. Remote Sens.*, *44*, 1093–1101.

Livesey, R. E., and W. Y. Chen (1983), Statistical field significance and its determination by Monte Carlo techniques, *Mon. Weather Rev.*, *111*, 46–59.

Madden, R. A., and P. R. Julian (1971), Description of the 40–50 day oscillation in the zonal wind in the tropical Pacific, *J. Atmos. Sci.*, *28*, 702–708.

Madden, R. A., and P. R. Julian (1994), Observations of the 40–50 day tropical oscillation-a review, *Mon. Weather Rev.*, *122*, 814–837.

Maloney, E. D., and D. L. Hartmann (2000), Modulation of hurricane activity in the Gulf of Mexico by the Madden-Julian Oscillation, *Science*, *287*, 2002–2004.

Mathews, A. J. (2000), Propagation mechanisms for the Madden Julian Oscillation, *Q. J. R. Meteorol. Soc.*, *126*, 2637–2651.

Miyoshi, Y., and H. Fujiwara (2006), Excitation mechanism of intraseasonal oscillation in the equatorial mesosphere and lower thermosphere, *J. Geophys. Res.*, *111*, D14108, doi:10.1029/2005JD006993.

Mo, K. C. (2000), The association between intraseasonal oscillations and tropical storms in the Atlantic Basin, *Mon. Weather Rev.*, *128*, 4097–4107.

Nakazawa, T. (1986), Intraseaonal variations in OLR in the tropics during the FGGE year, *J. Meteorol. Soc. Jpn.*, *64*, 17–34.

Park, C.-K., and S. D. Schubert (1993), Remotely forced intraseasonal oscillations over the tropical Atlantic, *J. Atmos. Sci.*, *50*, 89–103.

Sassi, F., M. Salby, H. C. Pumphrey, and W. G. Read (2002), Influence of the Madden-Julian Oscillation on upper tropospheric humidity, *J. Geophys. Res.*, *107*(D23), 4681, doi:10.1029/2001JD001331.

Schoeberl, M. R., et al. (2004), Earth observing system missions benefit atmospheric research, *Eos Trans. AGU*, *85*, 177.

Stanford, J. L., et al. (1993), Stratospheric circulation features deduced from SAMS constituent data, *J. Atmos. Sci.*, *50*, 226–246.

Tian, B., Y. L. Yung, D. E. Waliser, T. Tyranowski, L. Kuai, E. J. Fetzer, and F. W. Irion (2007), Intraseasonal variations of the tropical total ozone and their connection to the Madden-Julian Oscillation, *Geophys. Res. Lett.*, *34*, L08704, doi:10.1029/2007GL029451.

Waters, J. W., et al. (2006), The Earth Observing System Microwave Limb Sounder (EOS MLS) on the Aura satellite, *IEEE Trans. Geophys. Remote Sens.*, *44*, 1075–1092.

Zhang, C. (2005), Madden-Julian Oscillation, *Rev. Geophys.*, *43*, RG2003, doi:10.1029/2004RG000158.

Ziemke, J. R., and S. Chandra (2003a), A Madden-Julian Oscillation in tropospheric ozone, *Geophys. Res. Lett.*, *30*(23), 2182, doi:10.1029/2003GL018523.

Ziemke, J. R., and S. Chandra (2003b), La Nina and El Nino–induced variabilities of ozone in the tropical lower atmosphere during 1970–2001, *Geophys. Res. Lett.*, *30*(3), 1142, doi:10.1029/2002GL016387.

Ziemke, J. R., S. Chandra, B. N. Duncan, L. Froidevaux, P. K. Bhartia, P. F. Levelt, and J. W. Waters (2006), Tropospheric ozone determined from Aura OMI and MLS: Evaluation of measurements and comparison with the Global Modeling Initiative's Chemical Transport Model, *J. Geophys. Res.*, *111*, D19303, doi:10.1029/2006JD007089.

P. K. Bhartia, S. Chandra, M. R. Schoeberl, and J. R. Ziemke, NASA Goddard Space Flight Center, Greenbelt, MD 20771-0001, USA. (ziemke@jwocky.gsfc.nasa.gov)

L. Froidevaux and W. G. Read, NASA Jet Propulsion Laboratory, Pasadena, CA 91109, USA.

P. F. Levelt, Royal Dutch Meteorological Institute, NL-3730 AE De Bilt, Netherlands.